Measurement 199 (2022) 111538

Contents lists available at ScienceDirect

Measurement

journal homepage: www.elsevier.com/locate/measurement

# Thermal drift reduction in photodiode dosimeters with switching bias

I. Ruiz-García [a], J. Román-Raya [b], P. Escobedo [a], M. Andjelkovic [c], D. Guirado [d,e], A.J. Palma [a], M. A. Carvajal [a,*]

[a] ECsens, Department of Electronics and Computer Technology, Sport and Health University Research Institute (iMUDS-UGR), Research Centre for Information and Communications Technologies (CITIC-UGR), University of Granada, 18071 Granada, Spain
[b] Instituto de Investigación Biosanitaria, ibs.Granada. Hospital Universitario Virgen de las Nieves, Granada, Spain
[c] IHP – Leibniz-Institute für innovative Mikroelektronik, Frankfurt (Oder), Germany
[d] Instituto de Investigación Biosanitaria, ibs.Granada. Hospital Universitario Clínico San Cecilio, Granada, Spain
[e] CIBER de Epidemiología y Salud Pública (CIBERESP), Granada, Spain

ARTICLE INFO

*Keywords:*
PIN Photodiode
Dosimeter
Thermal compensation
Forward voltage

ABSTRACT

The effect of temperature on dosimetric measurements is a major limitation of solid-state dosimeters. This is especially true for PIN photodiode dosimeters, where the dark current depends exponentially on temperature. To minimize this effect, a compensation method is presented that relies on the diode structure itself without the need for an external sensor or device. During irradiation, the photodiode is periodically switched from reverse to forward polarization to determine the temperature of the device. This measurement is based on the linear dependence between the temperature and the forward voltage of the diode when it is operated at constant current. An electronic circuit implementing this procedure was developed and used for experimental characterization of the response to radiation of the BPW34S Si PIN photodiode. The proposed procedure reduced the uncertainty due to thermal drift by a factor of 7.5. In addition, an average dose rate sensitivity of $12 \pm 2$ nC/cGy was measured, with a sensitivity degradation below 2% for the irradiation cycle of 21.4 Gy performed under a 6 MV photon beam. We have shown that a p-n junction can be successfully used to compensate for the temperature effect on the dosimetric measurement.

## 1. Introduction

Radiotherapy is one of the most common and effective treatments for solid cancers. In radiotherapy, it is essential to adequately determine the absorbed dose to ensure a proper tumour cells damage while preserving healthy cells as much as possible. Ionization chambers are the most commonly used devices for radiotherapy dosimetry. The ionization chamber is connected to an electrometer both to apply the required electric field by means of a bias voltage and also to measure the charge induced by the radiation, integrating the current. This system presents some limitations compared to semiconductor-based systems, such as comparatively higher cost, larger size, and high voltage requirement for biasing. As an alternative or complement, some current-mode semiconductor devices have been studied for the same purpose, such as photodiodes and phototransistors [1–3]. Silicon diodes work in a similar way as ionization chambers. In this case, the detection volume is the depletion region, and it can operate in two different modes: photovoltaic mode, when the electric field for charge separation is internal, or photoconductive mode, when an electric field is externally applied. The induced photocurrent is usually measured with an external electrometer as well. This magnitude can be related to the radiation dose rate, and the absorbed dose is proportional to the integral of the current over the exposure time [4–6].

Some authors have proposed the use of low-cost commercial optoelectronic detectors such as light-dependent resistors (LDR) as dosimetry detectors [7–9]. The LDR operation is based on the resistivity change due to the generation of electron-hole pairs as a result of the absorption of photons. Other devices used in radiotherapy, particularly for in vivo dosimetry, are MOSFETs (metal–oxidesemiconductor field effect transistors). MOSFETs offer several advantages for dosimetry applications, such as immediate and non-destructive readouts, low power consumption, easy calibration, and reasonable sensitivity and reproducibility [10–13]. Because the sensitivity of MOSFET dosimeters in the unbiased mode is low, and at high dose rates the linearity of their response is

* Corresponding author.
*E-mail addresses:* isirg@ugr.es (I. Ruiz-García), juan.roman.raya.sspa@juntadeandalucia.es (J. Román-Raya), ajpalma@ugr.es (P. Escobedo), andjelkovic@ihp-microelectronics.com (M. Andjelkovic), dguirado@ugr.es (D. Guirado), pabloescobedo@ugr.es (A.J. Palma), carvajal@ugr.es (M.A. Carvajal).

https://doi.org/10.1016/j.measurement.2022.111538
Received 11 April 2022; Received in revised form 7 June 2022; Accepted 21 June 2022
Available online 28 June 2022
0263-2241/© 2022 Published by Elsevier Ltd.

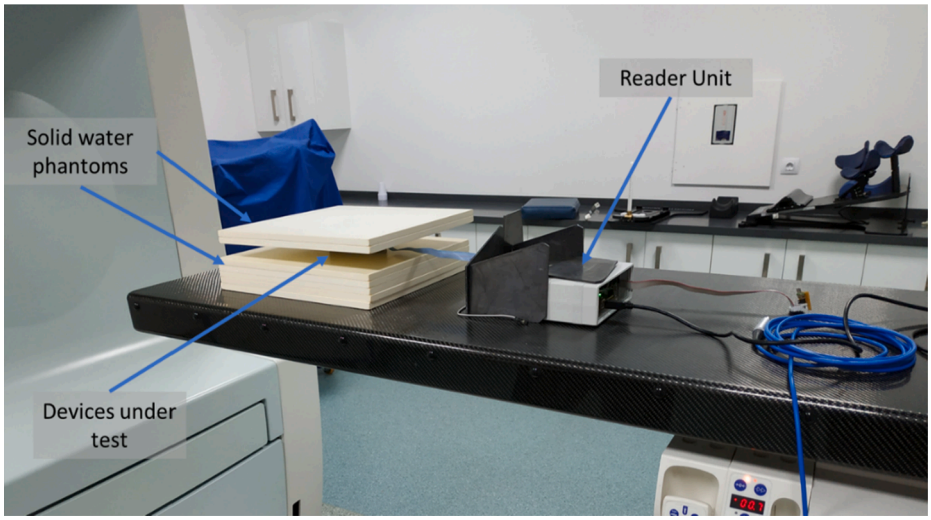


**Fig. 1.** Experimental setup for the dosimetric characterization of the photodiode radiation response. Solid water layers are shown under and over the box containing the devices under test.

reduced, efforts to increase the sensitivity of MOSFET dosimeters have involved their manufacture with a special technological process to achieve a thick gate oxide (more than 200 nm). The resulting devices are known as RADFETs (Radiation Field Effect Transistor) [14–16].

However, semiconductor-based systems generally present an important limitation due to their temperature dependence, hindering an accurate dose measurement. This issue has been tackled by some authors in different solid-state dosimeters. For thermal correction in RADFETs, different strategies have been described. The most direct one is to set it at the bias point with the minimum temperature coefficient, in the so-called drain current condition, $I_{ZTC}$ [17]. Another thermal compensation method is based on differential measurements of the source–drain voltage of two identical MOSFETs. These transistors are biased using the same current during readout but irradiated at different gate–source voltages. Consequently, they have different sensitivities to radiation, which produces different source–drain voltage shifts. Nevertheless, thermal fluctuation is the same in the two transistors and the difference is minimized by applying a differential measurement [18]. Another strategy was proposed using a custom read-out system applying two or three drain currents to the same RADFET [19]. Furthermore, the same authors developed a thermal compensation technique using the parasitic diode for DMOS transistor dosimeters [20].

In this work, based on a similar idea to the one used for thermal compensation of DMOS transistors, a PIN photodiode is thermally studied, and a thermal compensation method is hereby presented and applied. Our proposal consists in periodically measuring the forward voltage ($V_\gamma V_F$) as a method to measure the temperature of the device. This value is employed for the thermal correction of the reverse dark current ($I_S$), which is the baseline of the radiation-induced photocurrent and the main contributor to its thermal drift. Therefore, as a prerequisite, the temperature dependence of both the forward voltage [21–24] and the photodiode dark current must be accurately characterised. In short, the PIN photodiode will be forward biased for temperature measurement mode, and reverse biased for dose rate determination mode. Moreover, a thermal compensated read-out unit has been redesigned to implement the proposed procedure [25].

## 2. Materials and methods

PIN photodiode BPW34S (Vishay, Malvern, Pennsylvania, USA) was selected as the dosimetric sensor. The reason for this choice was that this optoelectronic device has already been characterised as radiation detector for irradiations typically applied in radiotherapy treatments, showing a promising response in terms of sensitivity and reproducibility [3,26]. Two experimental device characterizations were conducted: (i) a complete modelling of the dependence with the temperature in reverse (dark current) and under forward biasing, and (ii) its response to ionizing radiation in reverse biasing. In both cases, each device under test (DUT) was painted with black nail polish and, in addition, they were placed into a box to shield it from environmental light.

A total of eleven samples were employed for the thermal characterization. Six samples were divided in two groups of three devices. One group was used for the thermal modelling of forward biased DUT at constant current, and the other for the validation of the proposed model, respectively. Moreover, thermal dependence of the dark current under reverse biasing was measured in five samples. For temperature-controlled tests, samples were placed inside a climate chamber VCL4006 (Vötsch Industrietechnik, Balingen-Frommern, Germany). To monitor the temperature more accurately, a digital thermometer RS 408–6109 (Amidata S.A., Madrid, Spain) with an accuracy of 0.1 °C was placed inside the chamber close to the photodiodes. To minimize the infrared radiation produced by the chamber while heating, the photodiodes box was also covered with aluminium foil. Then, current–voltage characteristic curves were measured at different temperatures with the Semiconductor Analyzer B1500A (Agilent Technologies, Santa Clara, USA). To perform the thermal characterization, temperature sweeps from 10 to 35 °C in steps of 5 °C were conducted, and the photodiodes were forward biased in the range from 0 to 2 mA by the Semiconductor Analyser.

In the second step, the dosimetric characterization of the photodiodes was performed. Eight samples of the BPW34S were irradiated with a linear accelerator (LINAC) Siemens Artiste (Siemens Healthcare GmbH, Erlangen, Germany), placed at the “Hospital Universitario Clínico San Cecilio” (Granada, Spain). The photon beam was produced with an electric potential of 6 MV. DUTs were located in the radiation isocenter (at 100 cm away from the source) and were irradiated with a field size of 10x10 $cm^2$. To achieve the electronic equilibrium, two solid water phantoms of 1 cm each were placed over the DUT. In addition, five solid water phantoms were placed under the DUT, as Fig. 1 shows. The majority of radiation detectors, including PIN photodiodes, measure the energy inside the volume of matter by the charge created inside it. That is the reason why a suitable measurement must be done with the detector in electronic equilibrium condition, where the charge entering the volume by external process would be approximately equal to the loss of charge created by internal process [4].

With these irradiation conditions, in terms of delivered dose, one

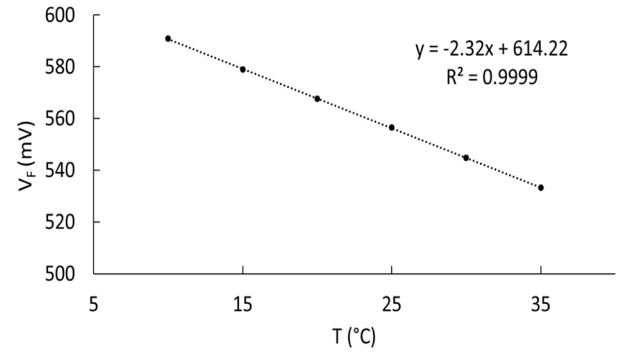


(a)

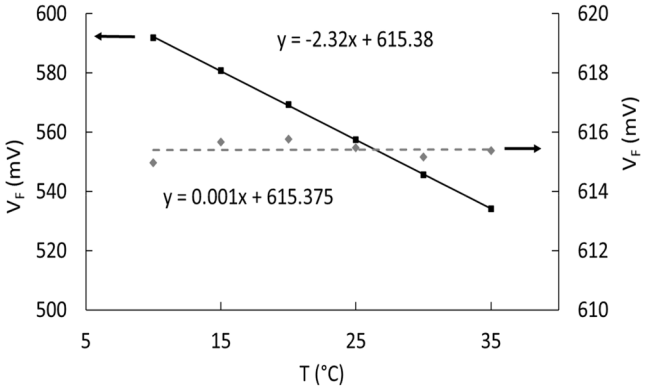


(b)

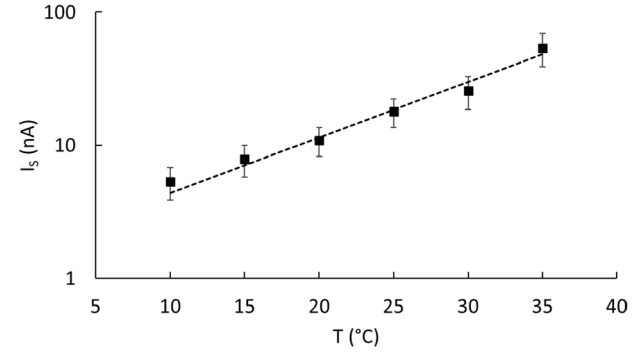


(c)

**Fig. 2.** (a) $V_F$ at constant drain current ($I_D$ = 1 mA) vs. temperature for the modelling group. Experimental data are shown with symbols and linear fitting with the dotted line. Average values of the three sensors are presented. Error bars are smaller than symbols (b) $V_F$ vs. temperature at 1 mA for the validation group of sensors. Black symbols and line are the experimental data and the linear fitting respectively, and grey ones represent the temperature correction given by the modelling from Fig. 2a. Error bars are smaller than symbols (c). Dark current, $I_S$, showing experimental data (squared symbols) and the exponential fitting (dotted line symbols) at reverse bias of 10 V.

monitor unit (MU) of the LINAC corresponds to 0.973 cGy (calibrated at 300 MU/min with a pulse duration of 3 μs and a pulse repetition frequency of 222 Hz). The constancy checks performed on the LINAC ensure that the absorbed dose per monitor unit varies less than 0.5% throughout the tests. Using this configuration and varying pulse repetition frequency, instantaneous dose rates of 50, 100, 150, 200, 250 and 300 MU/min (0.81 cGy/s, 1.62 cGy/s, 2.13 cGy/s, 3.24 cGy/s, 4.05 cGy/s, and 4.87 cGy/s respectively) were applied to characterize the photodiodes response to radiation. The 90-minute irradiation cycle consists of a six-step decreasing instantaneous dose rate staircase from 4.87 to 0.81 cGy/s, a six-step increasing instantaneous dose rate staircase from 0.81 to 4.87 cGy/s, and a last step of 0.81 cGy/s. Between each step, a period without irradiation of 2 min was applied. In all cases, each dose rate step duration was calculated to deliver a constant value of 200 MU.

To measure the induced photocurrent, photodiodes were always reverse biased at −10 V. To avoid electromagnetic interference on the photodiode's output current, the readout system was placed into the treatment room but out of the irradiation field. Moreover, the system was shielded by a 3-mm-thick lead layer to protect it from radiation and connected to a computer, placed outside of the treatment room, through an USB cable. More details of the experimental setup and conditions can be consulted elsewhere [26]. For both experimental characterizations, relative uncertainties were obtained as the quadratic propagation of experimental data and one standard deviation of each individual result. Data will be graphically presented as mean with a covering factor k = 1 (1 standard deviation).

## 3. Results and discussion

### 3.1. 3.1. Thermal compensation technique

Our proposal relies on the linear relationship between the forward voltage, $V_F$, of a p-n junction and temperature [27] as a means to monitor the device temperature. Let us consider the current–voltage curve of a forward biased diode:

$$I = I_s \hat{A} \cdot \exp(qV_F/2kT), \tag{1}$$

where $I$ is the junction current, $I_s$ is the saturation current, $q$ is the absolute value of the charge of an electron, $V_F$ is the diode forward voltage, $k$ is the Boltzmann constant and $T$ is the absolute temperature. It can be shown that the temperature-dependent voltage across the junction can be expressed as:

$$V_F = \frac{E_g}{q} - \frac{2kT}{q}(lnK - lnI), \tag{2}$$

where $E_g$ is the energy band gap for silicon at 0 K, and $K$ is a temperature independent constant. Therefore, when the diode is operated under constant current, the voltage is linearly dependent on temperature, with a typical slope around −2 mV/K.

Once this linear temperature coefficient has been modelled, just with the experimental measurement of $V_F$, temperature can be measured in the volume device at any time. Therefore, thermal drift of the dark current can be corrected with this calculated temperature. Provided the periodic $V_F$ monitoring, this methodology can be applied to monitor device temperature in real time. Therefore, both forward and reverse biasing must be alternatively applied to the device under irradiation to conduct this procedure as it will be explained below in the readout system description.

Thermal dependence of $V_F$ at constant current was measured by biasing at 1 mA to reduce device self-heating by Joule effect. In Fig. 2a, the linear dependence of $V_F$ with the temperature is clearly obtained for the modelling group. The average linear temperature coefficient, α, was calculated as the average of the thermal coefficient of the three photodiodes studied, resulting $\alpha = (-2.32 \pm 0.01)$ mV/K. Therefore, this linear model provides us an accurate determination of the device temperature, just measuring $V_F$, that is objectively simpler than measuring the temperature itself. Moreover, we get an additional advantage: this is the temperature in the detector volume. This thermal model has been validated with the validation group in Fig. 2b. In this Fig. 2b, both the average temperature dependence of the three diodes (black symbols) and their correction with the fitting from Fig. 2a are shown (grey symbols). On the other hand, Fig. 2c depicts, with squared symbols, the

**Table 1**
Modelling of $V_{\gamma F}$ and $I_S$ dependences with the temperature.

| | $V_F$ vs. $T$ | $I_S$ vs. $T$ |
|---|---|---|
| **Theoretical model** | $V_F = \alpha\hat{A}\cdot T + \beta$ | $I_S = A\hat{A}\cdot e^{B\bullet T}$ |
| **Fitting parameters** | $\alpha = (-2.32 \pm 0.01)$ mV/K$\beta =$ $(614 \pm 2)$ mV $R^2 = 0.9999$ | $A = (1.7 \pm 0.3)$ AB $=$ $(0.096 \pm 0.007)$ $K^{-1}$ $R^2 = 0.9977$ |

temperature dependence of the dark current measured in the same conditions as during irradiation, that is, with a reverse voltage of −10 V. We can see the expectable exponential behaviour according to the theoretical model of this parameter [28]. Fig. 2b also shows the excellent exponential fitting (dotted line) of experimental data. Both the theoretical models and the fitting parameters are shown in Table 1. These results will ensure an accurate temperature correction of the dark current and, therefore, of the baseline of the induced photocurrent of this device used as a dosimetric sensor, as it will be shown below. Moreover, we have to remark the fact that under irradiation, the induced photocurrent is in the hundreds of nA, which is negligible with respect to the forward current (1 mA) in the temperature measurement mode and, therefore, it has no effect in the temperature compensation procedure.

### 3.2. System description and operation

The described two-phase procedure, reverse- and forward-biasing of the PIN photodiode, has been periodically conducted throughout all the dosimetric characterisation previously described. This has provided a continuous and accurate monitoring of the device temperature and a real-time thermal drift compensation method. To do so, we have developed a dosimetric system consisting of a reader unit with the bias module, which is connected to a personal computer for data transfer and unit powering. This device is based on a previous design [20]. Fig. 3 shows the complete architecture of the reader unit, pointing out the selectable photodiode biasing. With this same purpose, the analog switch ADG419 (Analog Devices, Massachusetts, USA) has been included in the reader unit. Its purpose is to disconnect the sensors from the reverse bias voltage ($V_R$) and connect them between ground and current sink, thus allowing the measurement of the forward voltage. With this topology, it is possible to alternatively measure both $V_F$ and the induced photocurrent.

When the topology to measure induced current by radiation is selected by the microcontroller, the photodiode is biased at −10 V and the current generated is related to the dose rate (top signal path in Fig. 3a). After that, the reader unit switches to measure $V_F$. To do this, the analog switch disconnects the photodiodes photodiode from bias

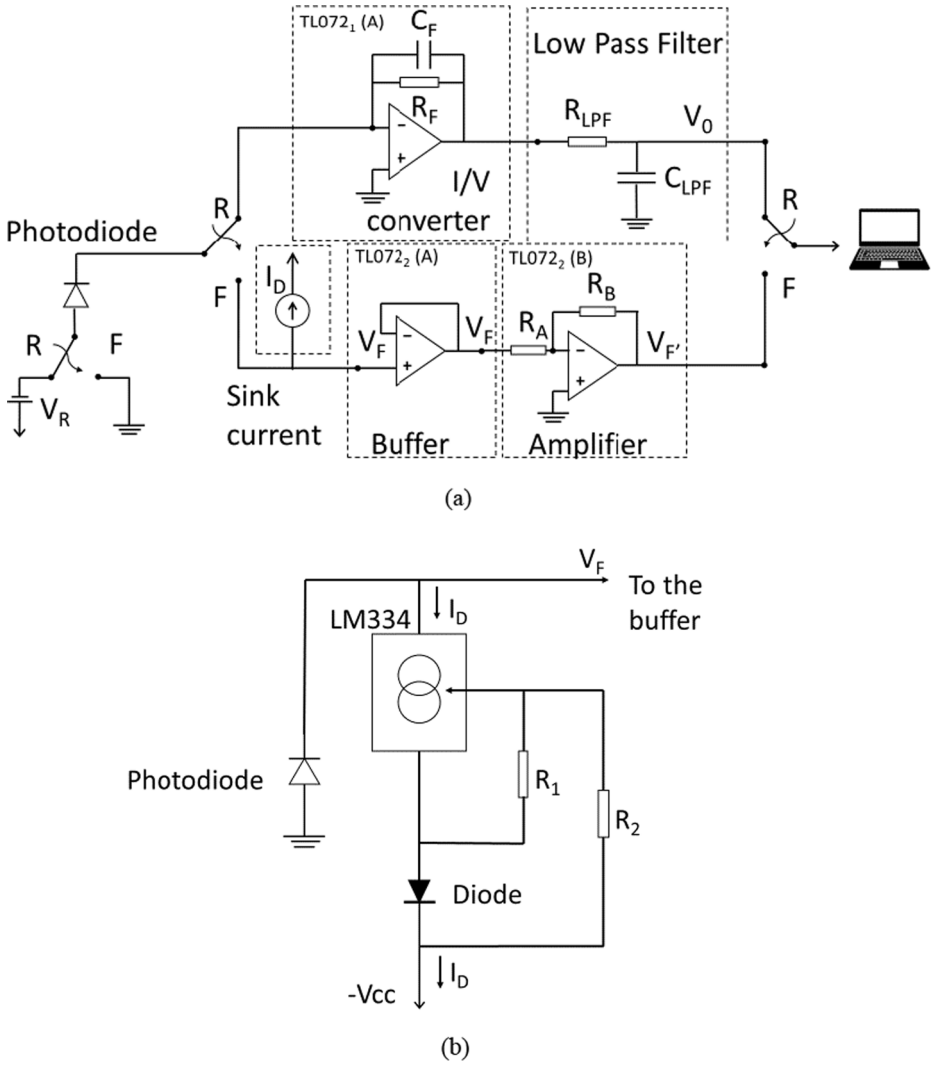


**Fig. 3.** (a) Schematic of the reader unit showing the signal path for forward bias (F) and for reverse bias and irradiation mode (R). In this circuit, the reverse voltage is $V_R$ = -10 V and forward current $I_D$ = 1 mA. Final connection to computer is also shown. (b) Current sink circuit for forward biasing the photodiode based on LM344 chip with compensation of the temperature effect.

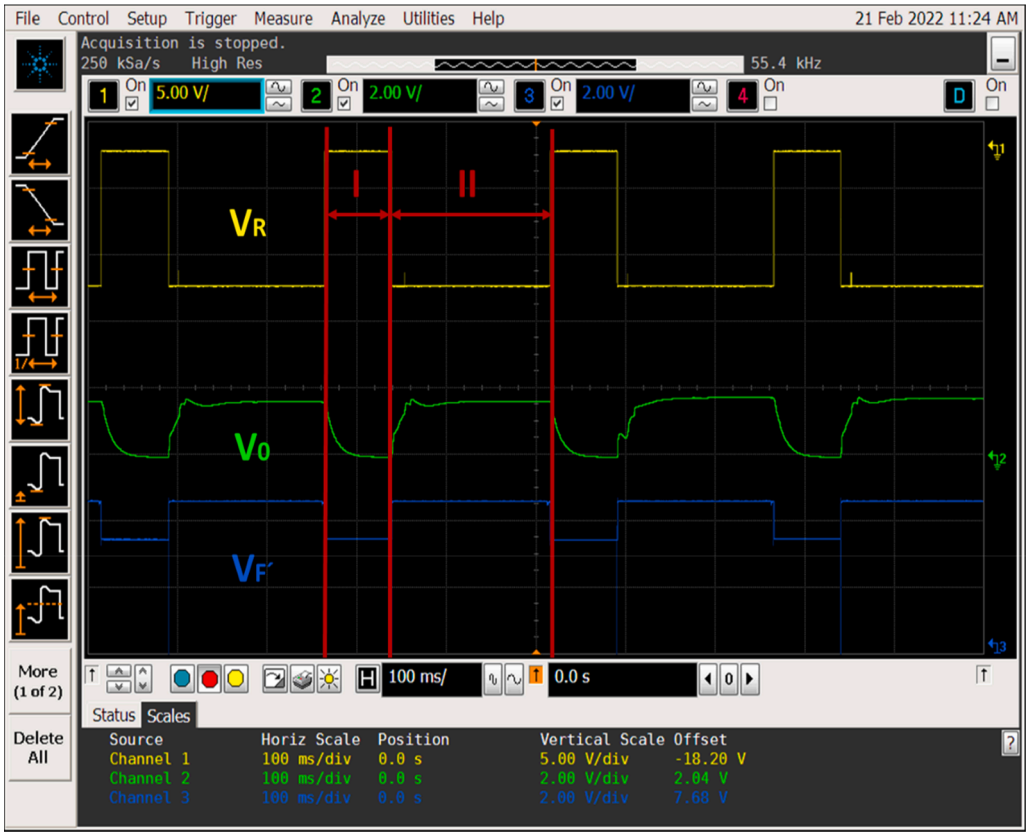


**Fig. 4.** Screenshot from an oscilloscope of the system operation. Yellow and blue lines show reverse and forward voltages respectively, that are applied in phases I and II. Phase I stands for temperature measurement in forward bias and phase II for photocurrent measurement, including compensation of the temperature effect. Green line, $V_{S0}$, is the output voltage in Fig. 3a.

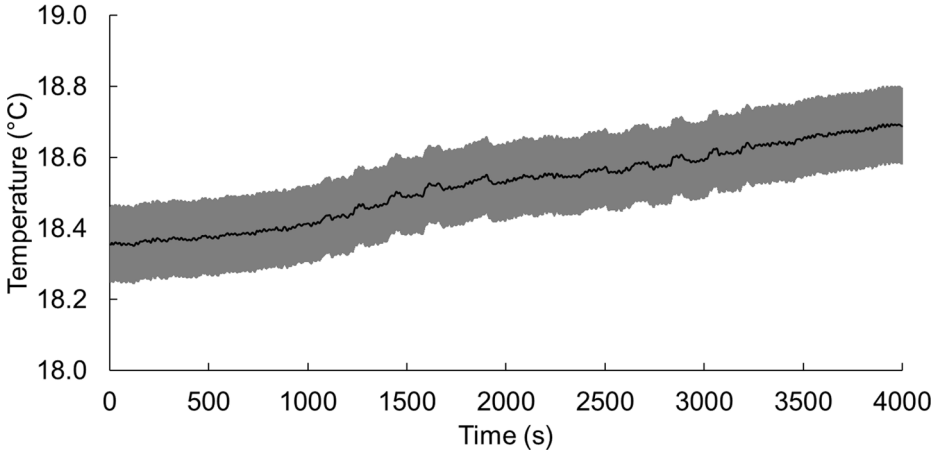


**Fig. 5.** Temperature drift of the sample #4 during the irradiation experiment with the proposed procedure. Shaded interval represents experimental data uncertainties (coverage factor k = 1).

voltage and I/V converter and connects them between ground and sink current. Now, $V_F$ is measured through the buffer and the amplifier, both based on the operational amplifier TL072 (Texas Instruments, Dallas, TX, USA) (bottom signal path in Fig. 3a). A configurable sink current designed with LM334 chip (Texas Instruments, Texas, USA) was also added to bias the photodiodes in the forward region (Fig. 3b). The current sink, $I_D$, was selected to minimize the temperature coefficient (LTC) of the LM334 [29]. The circuit shown in Fig. 4 balances the positive LTC of the LM334 with the negative LTC of the forward-biased silicon diode. The diode used was 1 N4148 (Vishay, Malvern, Pennsylvania, USA), and the resistors $R_1$ and $R_2$ were configured to select the desired current, 3.3 kΩ and 33kΩ, respectively. With this configuration $I_D$ was set to 1 mA, to reduce diode self-heating.

The two operation modes can be observed in the timing chart depicted in Fig. 4. Time period of this two-phase procedure was 1 s to ensure signal stabilisation. During phase I, the photodiode is forward-biased to measure $V_F$ and then, to calculate the device temperature. Afterwards, the dosimetric behaviour can be measured with the photodiode reverse-biased in phase II.

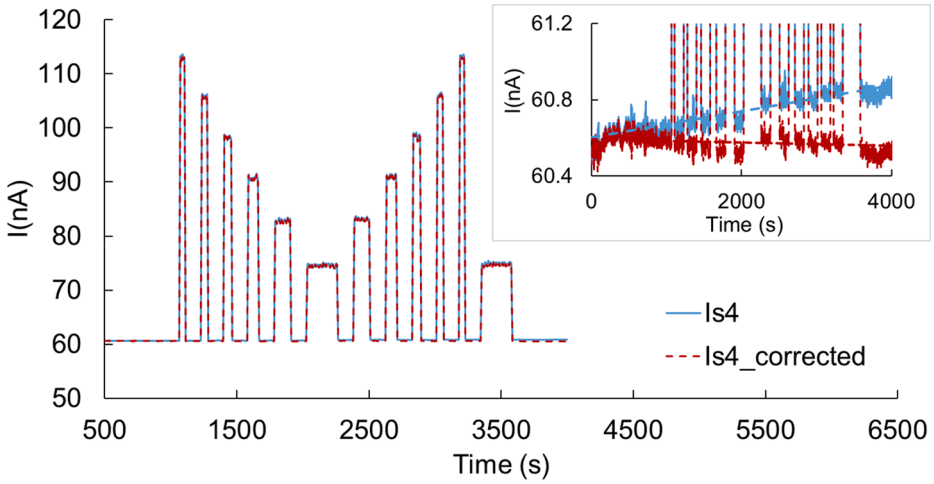


**Fig. 6.** Experimental photocurrent during the dosimetric characterization of the sample #4 showing the proposed complete irradiation cycle. Inset shows the zoomed dark current before ($I_{s4}$, blue dots) and after ($_{Is4\_corrected}$, red dots) thermal compensation.

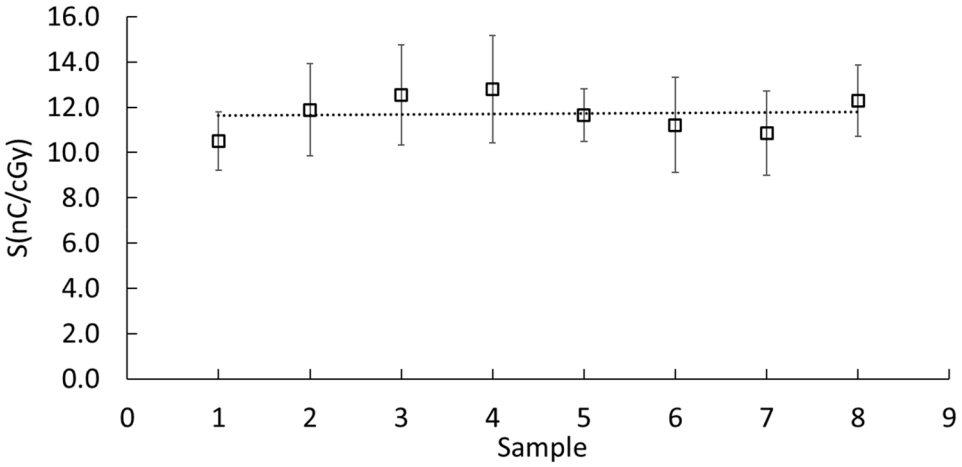


**Fig. 7.** Photodiode sensitivity to instantaneous dose rate. Experimental data uncertainties correspond to a coverage factor k = 1. Line shows the average sensitivity.

### 3.3. Thermal compensation of the response to the radiation

Using the procedure of temperature determination described in Section 3.1, Fig. 5 shows the temperature drift of the sample #4 under the irradiation experiment described above. As mentioned above, acquisition frequency of the device temperature was 1 Hz, demonstrating that it is suitable to monitor this slow changing magnitude in this experimental condition. A heating of 0.35 °C can be measured due to the energy deposition by the photon beam and self-heating. Considering the exponential temperature trend of the dark current, this thermal drift results in a non-negligible baseline drift. Therefore, it should be corrected to obtain an accurate dose rate determination.

Fig. 6 displays the photodiode current of the complete irradiation cycle of the sample #4. Fig. 6 inset zooms the baseline data, that is, the dark current. Blue dots depict the uncompensated baseline with a total drift of 0.20nA. This value represents a relative error of 1.5% in the worst case (for the lower dose rate, 0.81 cGy/s). Once our compensation method is applied, red dots are obtained, resulting in a maximum relative error of 0.2%, thus achieving a significant reduction of the baseline linear thermal drift by a factor of 7.5. As a consequence, these figures prove the effectiveness of the proposed procedure by taking advantage of a p-n junction as an accurate and linear temperature sensor. With this temperature correction, the photodiode sensitivity, S, was obtained as the slope of the linear fit of the induced current (nA) as a function of dose

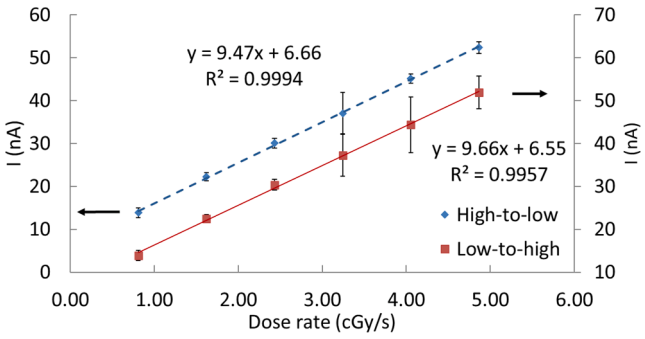


**Fig. 8.** Photocurrents versus high to low (diamond symbols) and low to high (square symbols). Lines show the linear tendencies. Experimental data uncertainties are shown with bars (coverage factor k = 1).

rate (cGy/s) for each device. Fig. 7 shows the radiation sensitivity of each irradiated photodiode. The average sensitivity can be calculated, obtaining S = 12 ± 2 nC/cGy (coverage factor k = 1). This result is similar to the previously obtained value of 13.8 ± 0.4 nC/cGy [26]. The slightly lower measured sensitivity can be explained because the photodiode is forward biased for a fraction of time to implement the temperature compensation procedure, instead of being always reversed

**Table 2**
Modelling of sensitivity with dose rate.

| | High to low dose rate $A \bullet x + B$ | Low to high dose rate $C \bullet x + D$ |
|---|---|---|
| **Fitting parameters** | A = (9.47 ± 0.11) nC/cGyB = (6.7 ± 0.3) nA | C = (9.7 ± 0.3) nC/cGyD = (6.6 ± 0.5) nA |

while the irradiation. Therefore, when the device is not reverse biased, its sensitivity decreases because of a lower capability of electron-hole separation before recombination, generating lower photocurrent.

As shown in Fig. 6, to determine the repeatability and stability of the sensor response, high to low and low to high dose rate irradiation cycles were applied and sensitivity degradation was found below 2% in the dose range up to 21.4 Gy. The degradation was calculated as the relative decrease of both slopes in percentage in the whole irradiation cycle (see Fig. 8). Table 2 shows the fitting parameters of curves from Fig. 8, obtaining the mentioned slight decrease of the sensitivity in the second part of the irradiation cycle (from low to high dose rate).

## 4. Conclusions

A method for thermal compensation of radiation-induced current in photodiodes has been presented and experimentally tested. It is based on the linear dependence between temperature and forward voltage ($V_{\gamma F}$) of a p-n junction. In fact, measuring this forward voltage, we can monitor the device temperature and correct the highly thermal sensitive dark current. It has the advantage that no external sensors are needed to obtain the temperature. To do that, only a few modifications have been introduced in the reader unit previously developed by our research group.

To check the algorithm, the BPW34S Si PIN photodiode was used as a current-mode radiation sensor. Applying the compensation algorithm implemented in the reader, the thermal drift of the photodiode dark current was reduced from 1.5% to 0.2% for the lower dose rate. Moreover, with an accumulated dose of 21.4 Gy of photon beams of 6 MV, a sensitivity degradation below 2% and an average sensitivity of 12 ± 2 nC/cGy were obtained, which is in agreement with previous results. Therefore, the procedure presented in this work is suitable to model and reduce the thermal dependence in measured radiation-induced current of photodiodes.

### *CRediT authorship contribution statement*

**I. Ruiz-García:** Writing – review & editing. **J. Román-Raya:** Writing – review & editing. **P. Escobedo:** Writing – review & editing. **M. Andjelkovic:** Writing – review & editing, Data curation, Formal analysis. **D. Guirado:** Writing – review & editing, Data curation, Formal analysis, Methodology. **A.J. Palma:** Conceptualization, Methodology, Writing – review & editing, Supervision. **M.A. Carvajal:** Conceptualization, Investigation, Writing – review & editing, Supervision.

## Declaration of Competing Interest

The authors declare that they have no known competing financial interests or personal relationships that could have appeared to influence the work reported in this paper.

## Acknowledgments

This research has been partially funded by Junta de Andalucía (Spain), projects numbers PI-0505-2017 FEDER/Junta de Andalucía-Consejería de Economía y Conocimiento Project B-TIC-468-UGR18, Proyecto del Plan Nacional I + D: PID2019-104888 GB-I00 and Proyectos I + D + i Junta de Andalucía 2018: P18-RT-3237. This work was also conducted in the framework of H2020 ELICSIR project (grant No. 857558). P. Escobedo thanks grant IJC2020-043307-I funded by MCIN/AEI/ 10.13039/501100011033 and by "European Union Next-GenerationEU/PRTR".

## References

[1] L.A.P. Santos, E.F. da Silva Jr, E. Vilela, Filtered X Ray Beam Dosimetry from 10–3 to 102 Gy Dose Range by using Phototransistors, Radiat. Prot. Dosimetry. 101 (2002) 145–148, https://doi.org/10.1093/oxfordjournals.rpd.a005956.
[2] C. Romei, A.D. Fulvio, C.A. Traino, R. Ciolini, F. d'Errico, Characterization of a low-cost PIN photodiode for dosimetry in diagnostic radiology, Phys. Med. 31 (2015) 112–116, https://doi.org/10.1016/j.ejmp.2014.11.001.
[3] M. Andjelkovic, G. Ristic, Feasibility study of a current mode gamma radiation dosimeter based on a commercial PIN photodiode and a custom made auto-ranging electrometer, Nucl. Technol. Radiat. Prot. 28 (1) (2013) 73–83.
[4] G.F. Knoll, Radiation detection and measurement, 3rd Ed., John Wiley & Sons Inc, 2000.
[5] J. Barthe, Electronic dosimeters based on solid state detectors, Nucl. Instrum. Methods Phys. Res. Sect. B Beam Interact. Mater. At. 184 (2001) 158–189, https://doi.org/10.1016/S0168-583X(01)00711-X.
[6] A.B. Rosenfeld, Electronic dosimetry in radiation therapy, Radiat. Meas. 41 (2006) 134–153, https://doi.org/10.1016/j.radmeas.2007.01.005.
[7] I.S. Deev, The Use of Cadmium Sulphide Photo-Conductors in Radiation Dosimetry, J. Nucl. EnergyPart BReactor Technol. 1 (1960) 204–210, https://doi.org/10.1016/s0368-3273(15)30029-8.
[8] F.A.S. Soliman, H.A. Ashry, Radiation effects on non-linear resistances, J. Mater. Sci. Mater. Electron. 4 (1993) 293–300, https://doi.org/10.1007/BF00179227.
[9] J. Román-Raya, I. Ruiz-García, P. Escobedo, A.J. Palma, D. Guirado, M.A. Carvajal, Light-dependent resistors as dosimetric sensors in radiotherapy, Sens. Switz. 20 (6) (2020) 1568.
[10] M. Soubra, J. Cygler, G. Mackay, Evaluation of a dual bias dual metal oxide-silicon semiconductor field effect transistor detector as radiation dosimeter, Med. Phys. 21 (1994) 567–572, https://doi.org/10.1118/1.597314.
[11] A. Holmes-Siedle, L. Adams, RADFET: A review of the use of metal-oxide-silicon devices as integrating dosimeters, Int. J. Rad. Appl. Instr. C. Radiat. Phys. Chem. 28 (1986) 235–244, https://doi.org/10.1016/1359-0197(86)90134-7.
[12] R.C. Hughes, D. Huffman, J.V. Snelling, T.E. Zipperian, A.J. Ricco, C.A. Kelsey, Miniature radiation dosimeter for in vivo radiation measurements, Int. J. Radiat. Oncol. 14 (1988) 963–967, https://doi.org/10.1016/0360-3016(88)90019-3.
[13] R.A. Price, C. Benson, M.J. Joyce, K. Rodgers, Development of a RadFET linear array for intracavitary in vivo dosimetry during external beam radiotherapy and brachytherapy, - IEEE Trans, Nucl. Sci. 51 (2004) 1420–1426, https://doi.org/10.1109/TNS.2004.832570.
[14] D. Georg, B.D. Ost, M.-T. Hoornaert, P. Pilette, J.V. Dam, M.V. Dycke, D. Huyskens, Build-up modification of commercial diodes for entrance dose measurements in 'higher energy' photon beams, Radiother. Oncol. 51 (1999) 249–256, https://doi.org/10.1016/S0167-8140(99)00058-4.
[15] V. Panettieri, M.A. Duch, N. Jornet, M. Ginjaume, P. Carrasco, A. Badal, X. Ortega, M. Ribas, Monte Carlo simulation of MOSFET detectors for high-energy photon beams using the PENELOPE code, Phys. Med. Biol. 52 (2006) 303–316, https://doi.org/10.1088/0031-9155/52/1/020.
[16] M.A. Carvajal, S. García-Pareja, D. Guirado, M. Vilches, M. Anguiano, A.J. Palma, A.M. Lallena, Monte Carlo simulation using the PENELOPE code with an ant colony algorithm to study MOSFET detectors, Phys. Med. Biol. 54 (2009) 6263–6276, https://doi.org/10.1088/0031-9155/54/20/015.
[17] M. Osullivan, A. Kelleher, J. Ryan, B. Oneill, B. Lane, Temperature compensation of PMOS dosimeters, in: AA(University Coll., Cork (Ireland).), AB(University Coll., Cork (Ireland).), AC(University Coll., Cork (Ireland).), AD(University Coll., Cork (Ireland).), AE(University Coll., Cork (Ireland).), 1991: pp. 281–285. https://ui.adsabs.harvard.edu/abs/1991ESASP.313..281O.
[18] I. Thomson, Direct reading dosimeter, EP0471957A2, 1991.
[19] M.A. Carvajal, A. Martínez-Olmos, D.P. Morales, J.A. Lopez-Villanueva, A. M. Lallena, A.J. Palma, Thermal drift reduction with multiple bias current for MOSFET dosimeters, Phys. Med. Amp Biol. 56 (2011) 3535–3550, https://doi.org/10.1088/0031-9155/56/12/006.
[20] M.A. Carvajal, M.S. Martínez-García, D. Guirado, J. Banqueri, A.J. Palma, Dose verification system based on MOS transistor for real-time measurement, Sens. Actuators Phys. 247 (2016) 269–276, https://doi.org/10.1016/j.sna.2016.06.009.
[21] A. Szmyrka-Grzebyk, L. Lipiński, Low temperature current - voltage characteristics of silicon diodes used as thermometers, Cryogenics. 33 (1993) 222–225, https://doi.org/10.1016/0011-2275(93)90141-A.
[22] R.O. Ocaya, A linear, wide-range absolute temperature thermometer using a novel p–n diode sensing technique, Measurement. 46 (2013) 1464–1469, https://doi.org/10.1016/j.measurement.2012.12.008.
[23] R.O. Ocaya, An experiment to profile the voltage, current and temperature behaviour of a P-N diode, Eur. J. Phys. 27 (2006) 625–633, https://doi.org/10.1088/0143-0807/27/3/015.
[24] G.C.M. Meijer, Thermal sensors based on transistors, Sens. Actuators. 10 (1986) 103–125, https://doi.org/10.1016/0250-6874(86)80037-3.
[25] M.A. Carvajal, F. Simancas, D. Guirado, M. Vilches, A.M. Lallena, A.J. Palma, A compact and low cost dosimetry system based on MOSFET for in vivo radiotherapy, Sens. Actuators Phys. 182 (2012) 146–152, https://doi.org/10.1016/j.sna.2012.05.024.

[26] I. Ruiz-García, J. Román-Raya, J. Banqueri, A.J. Palma, D. Guirado, M.A. Carvajal, Commercial photodiodes and phototransistors as dosimeters of photon beams for radiotherapy, Med. Phys. 48 (2021) 5440–5447, https://doi.org/10.1002/mp.14921.
[27] J. Fraden, Handbook of Modern Sensors, 2nd Edition, Springer, New York, 1996.
[28] S.M. Sze, Physics of Semiconductor devices, John Wiley & Sons, New York, 1969.
[29] T. Instruments, LM134/LM234/LM334 3-Terminal Adjustable Current Sources, (2013). https://www.ti.com/lit/ds/symlink/lm134.pdf?ts=1637595584814.